# Racemic Amino Acid Piezoelectric Transducer

Sarah Guerin,[1,2,*] Joseph O'Donnell,[1,2] Ehtsham U. Haq,[1,2] Cian McKeown,[1,2] Christophe Silien,[1,2]
Fernando M. F. Rhen,[1,2] Tewfik Soulimane,[2,3] Syed A. M. Tofail,[1,2] and Damien Thompson[1,2]
[1]*Department of Physics, University of Limerick, Limerick V94 T9PX, Ireland*
[2]*Bernal Institute, University of Limerick, Limerick V94 T9PX, Ireland*
[3]*Department of Chemical Sciences, University of Limerick, Limerick V94 T9PX, Ireland*

(Received 8 July 2018; revised manuscript received 5 December 2018; published 29 January 2019)

Single crystal *L*-amino acids can exhibit technologically useful piezoelectric and nonlinear optical properties. Here we predict, using density functional theory, the piezoelectric charge and strain and voltage tensors of the racemic amino acid *DL* alanine, and use the modeling data to guide the first macroscopic and nanoscopic piezoelectric measurements on *DL*-alanine single crystals and polycrystalline aggregates. We demonstrate voltage generation of up to 0.8 V from *DL*-alanine crystal films under simple manual compression, twice as high as other amino acid crystals. Our results suggest that net molecular chirality is not a prerequisite for piezoelectric behavior in organic crystals. The transducer presented herein demonstrates that *DL*-alanine crystals can be used in applications such as temperature and force measurement in biosensors, data storage in flexible electronic devices, and mechanical actuation in energy harvesters.

DOI: 10.1103/PhysRevLett.122.047701

Piezoelectricity, the linear conversion of mechanical energy into electrical energy and vice versa, is a property of noncentrosymmetric crystals and manifests in inorganic materials, such as quartz ($SiO_2$) [1], lead zirconium titanate (PZT) [2], lithium niobate ($LiNbO_3$) [3], and zinc oxide (ZnO) [4], and in polymers containing crystallized regions such as polyvinylidene-fluoride [5]. Strong polarization in piezoelectric single crystals [1,6] and ceramics [7,8] creates a larger piezoelectric response than in polymers [9,10], with the disadvantage of being less flexible [11]. Biomolecules provide a promising alternative source of piezoelectric [12] and pyroelectric [13] crystals, which could potentially outperform and outlive currently used materials [14,15].

The potential of biomolecular piezoelectricity is emphasised in the work of Kholkin and co-workers as regards glycine crystal structures [16–18] and the peptide diphenylalanine [19,20], and also Li and co-workers whose work has focused on piezoelectricity of biological tissues [21,22], most notably elastin [23]. However, there has been a lack of theoretical and experimental studies on amino acid crystals outside of the three glycine polymorphs, in particular, the two piezoelectric racemic amino acids, namely, *DL* alanine and *DL* tyrosine [24]. We present this study as the development and characterization of a technologically useful, biocompatible energy harvester vs the tangential area of physiological piezoelectricity addressed in a number of works by Li and co-workers and ourselves [21–23,25,26].

The major advantage of using soft biological materials, such as amino acids, for energy harvesting applications is their relatively low dielectric constants ($\varepsilon_r$) [27,28]. While materials such as PZT and PMN-PT have much higher piezoelectric strain constants ($d_{ij}$), they also have much higher dielectric constants [2,29]. The piezoelectric voltage constant ($g_{ij}$, measured in V m/N) is inversely proportional to the dielectric constant [30],

$$g_{ij} = \frac{d_{ij}}{\varepsilon_{ii}} = \frac{e_{ij}}{c_{jj}\varepsilon_{ii}} \tag{1}$$

where $e$ is the piezoelectric charge constant, $d$ is the piezoelectric strain constant, $g$ is the piezoelectric voltage constant, $c$ is the elastic stiffness constant, and $\varepsilon$ is the dielectric constant. Here $i$ and $j$ are the direction of the electromechanical applied stimulus and response, respectively.

This means amino acid crystals (and biological materials generally of $\varepsilon = 2$–$3$) with modest $d_{ij}$ values of 1–10 pC/N (or in alternative units, pm/V) are capable of voltage outputs as high as inorganic ceramics. For example, bacterial phage viruses have piezoelectric voltage constants of approximately 0.2 V m/N [31,32], comparable to the voltage constants of currently used inorganic materials such as PZT-based ceramics (0.25 V m/N) [33] and Bismuth Triborate ($BiB_3O_6$) crystals (0.54 V m/N) [34]. We recently showed that amino acid microcrystals can exhibit larger energy densities [12] and demonstrated their growth on flexible substrates [12], which makes them suitable for *in vivo* energy harvesting and flexible motion sensing [35,36]. Unlike electroactive polymers, these biological crystals do not require high temperature poling to induce

© 2019 American Physical Society

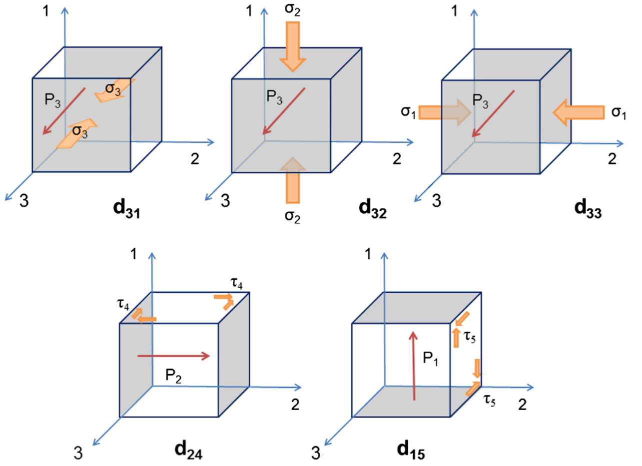

FIG. 1. Relationship between longitudinal ($\sigma$) and shear ($\tau$) stress and corresponding piezoelectric polarization ($P$) acting along arbitrarily chosen mutually orthogonal 1-2-3 axes for the five piezoelectric strain constants of *DL*-alanine single crystals, $d_{31}$, $d_{32}$, $d_{33}$, $d_{24}$, and $d_{15}$. Gray shading indicates the corresponding surfaces on which the electrodes are contacted to measure the polarization.

TABLE I. Predicted piezoelectric constants for *DL*-alanine amino acid single crystals.

Charge tensor (C/m$^2$)

$$\begin{pmatrix} 0 & 0 & 0 & 0 & 0.08 & 0 \\ 0 & 0 & 0 & 0.15 & 0 & 0 \\ 0.02 & -0.02 & 0.68 & 0 & 0 & 0 \end{pmatrix}$$

Strain tensor (pm/V)

$$\begin{pmatrix} 0 & 0 & 0 & 0 & 7.95 & 0 \\ 0 & 0 & 0 & 17.75 & 0 & 0 \\ 0.91 & -1.09 & 10.34 & 0 & 0 & 0 \end{pmatrix}$$

Voltage tensor (V m/N)

$$\begin{pmatrix} 0 & 0 & 0 & 0 & 0.39 & 0 \\ 0 & 0 & 0 & 0.82 & 0 & 0 \\ 0.04 & -0.05 & 0.47 & 0 & 0 & 0 \end{pmatrix}$$

a piezoelectric response via creation of aligned dipoles using high external fields [37].

Amino acids typically crystallize in orthorhombic and monoclinic space groups [38,39]. All amino acids except glycine form stereoisomers (enantiomers) around the central $\alpha$-carbon atom, meaning they can occur in *L* and *D* forms. Piezoelectricity has been confirmed qualitatively in *DL*-alanine single crystals [24], but never quantified. Here we have used density functional theory (DFT) to predict the complete piezoelectric tensors of the racemic mixture *DL*-alanine single crystals, using which we measured a longitudinal piezoelectric response of up to 5 pC/N in transducing crystal films and generated open circuit voltages as large as 0.8 V by manually compressing *DL*-alanine films.

*DL* alanine crystallizes with orthorhombic crystal symmetry that gives a nonzero longitudinal $d_{33}$ constant together with two transverse constants $d_{31}$ and $d_{32}$ and two shear constants $d_{24}$ and $d_{15}$ (Fig. 1). Table I shows the predicted piezoelectric charge and strain and voltage tensors for *DL* alanine. We note the relatively large predicted $e_{33}$ charge constant of 0.68 C/m$^2$, comparable to the highest predicted charge constant in glycine crystals of 0.81 C/m$^2$ [12]. This longitudinal piezoelectricity manifests as a dipole moment along the three axis of the crystal, as shown in Fig. 2(a). Applying a force along this axis will amplify or dampen the equilibrium polarization.

We can compare the computed maximum strain constants in Table I of up to 18 pm/V to our recently calculated, much smaller piezoelectric constants for *L*-alanine single crystals, in the range of 4–6 pC/N [26] (experimental values are similar, ranging from 2 to 4 pC/N) [40]. The elastic stiffness constants of *DL* alanine range from 7 to 67 GPa (Supplemental Material Table S1 [41]) and are almost identical to those of *L* alanine. *L*-alanine molecules pack as antiparallel layers [42], whereas in *DL* alanine the layers are parallel, alternating between *L*

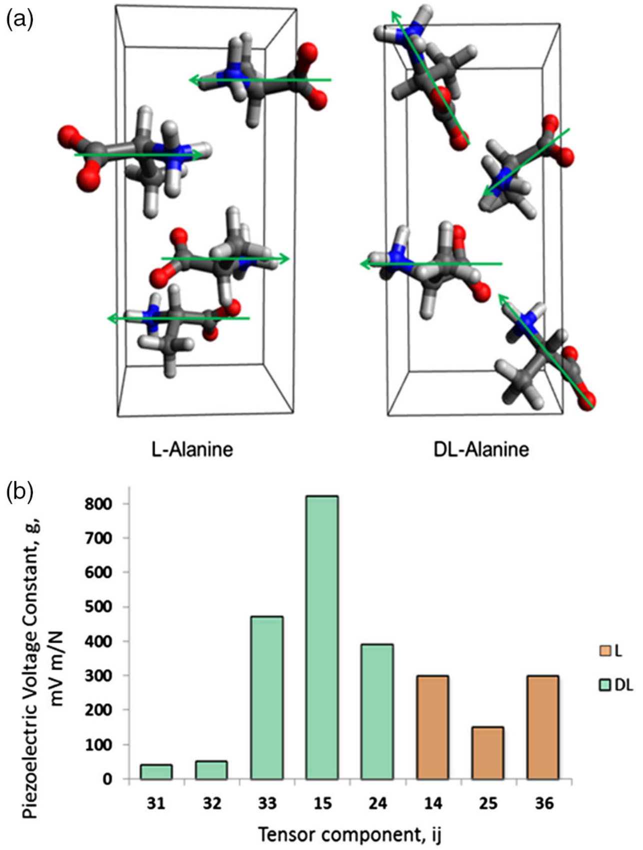

FIG. 2. (a) Crystal packing controls the orientation of alanine molecular dipoles (green arrows) in the unit cell, which determines the magnitude and direction of the corresponding piezoelectric responses. Molecules are shown with carbon atoms colored gray, hydrogen atoms in white, oxygen atoms in red, and nitrogen atoms in blue. (b) Comparison of the piezoelectric voltage constants of *L* and *DL* alanine, showing that both the longitudinal and shear response of the racemic mixture exceed that of the *L* enantiomer.

and *D* isomers. This results in different hydrogen bonding patterns and so different supramolecular packing and net dipole vectors [43]. In *L* alanine, the dipole vectors sum to zero, resulting in no net polarization in the unit cell and no longitudinal piezoelectricity. By contrast, the parallel packing in *DL* alanine means that the dipole vectors all point along the same direction [42], and the net polarization in the unit cell gives rise to both the longitudinal and transverse piezoelectric responses in the racemic crystal. Furthermore, this shows that net molecular chirality is not a prerequisite for piezoelectric behavior in organic crystals, building on previous studies of piezoelectricity in the achiral glycine polymorphs [12,44–46].

Predicted *DL*-alanine dielectric constants are typical for amino acid crystals [12,28] with an average value of 2.4 (unitless, Table S1). The low permittivities of amino acid crystals give high predicted piezoelectric voltage constants, with $g_{33}$, $g_{24}$, and $g_{15}$ all exceeding the maximum voltage constants measured in PZT ceramics (0.25 V m/N) [33] and $g_{24}$ exceeding that of bismuth triborate crystals (0.54 V m/N) [34]. This suggests that *DL*-alanine crystals are capable of generating technologically useful voltages under applied stress, within the limit of the lower fracture point of organic crystals compared to piezoceramics [47,48]. The predicted $d_{33}$ constant of 10.3 pm/V is as large as predicted and measured [12] for rhombohedral $\gamma$-glycine crystals.

After a range of growth conditions were tested (see Supplemental Material [49]), crystals were grown following the method of Hod *et al.* [50] in 25% isopropyl alcohol. This resulted in high density films of *DL*-alanine single crystal needles (Fig. S2), which could be tested for an average longitudinal piezoelectric response using a commercial $d_{33}$ piezometer. The crystal packing in the dense *DL*-alanine films was characterized using transmission x-ray diffraction and scanning electron microscopy (see Supplemental Material [58]).

*DL*-alanine crystalline films dropcast onto Cu substrates gave an average $d_{33}$ measurement of +4.1 and −3.9 pC/N, with the polarity change on inverting the sample confirming a genuine longitudinal piezoelectric response. The maximum recorded piezoelectric response for films was 4.8 pC/N, which is double that measured for samples on ITO glass (see SI) and the magnitudes of the positive and negative measurements are in good agreement. Table II shows five sets of piezoelectric measurements carried out at different positions along the polycrystalline aggregate films on five copper samples. The five points measured were off center and report local piezoelectric responses on the surface.

The highest local piezoresponse is 3.5 pC/N, with average values ranging from 1.1 to 2.6 pC/N. Percentage standard deviations across each film are in the range of 6%–33%. The standard deviation between films is similar in the upright (37%) and inverted (34%) configurations. We note that the piezoelectric response across each film is sensitive to small changes in the measurement zone (1–5 in Table II). The highest recorded measurements in Table II are close to the average value (4 pC/N) of the three predicted orthogonal responses for *DL*-alanine single crystals when stressed along the three axis (Table I). This value is similar to the piezoelectric constants of zinc oxide [4] and aluminium nitrate [61] and double that of *X*-cut quartz [1]. The different orientations of the crystals in the film, as evidenced by XRD and SEM, indicate that different faces of the crystals are in contact with the piezometer electrodes, resulting in a combined $d_{31}$, $d_{32}$, and $d_{33}$ response that varies from point to point. Because of the degree of randomness in the crystal growth, all three $d_{31}$, $d_{32}$, and $d_{33}$ constants may contribute to the measured piezoelectric response, suggesting that the highest predicted single crystal $d_{33}$ constant of 10.3 pC/N is diluted by the orthogonal responses.

TABLE II. Local piezoelectric measurements made on *DL*-alanine crystals grown on copper. Units are in pC/N.

| Film | | Position 1 | 2 | 3 | 4 | 5 | Average |
|---|---|---|---|---|---|---|---|
| A | Upright | 2.47 | 2.60 | 3.19 | 3.50 | 1.45 | 2.6 ± 0.8 |
| | Inverted | −2.45 | −2.49 | −3.30 | −2.49 | −1.46 | −2.4 ± 0.7 |
| B | Upright | 1.95 | 1.95 | 2.21 | 2.05 | 1.90 | 2.0 ± 0.1 |
| | Inverted | −1.96 | −2.12 | −1.67 | −1.36 | −1.95 | −1.8 ± 0.3 |
| C | Upright | 1.58 | 1.17 | 1.15 | 1.17 | 0.99 | 1.2 ± 0.2 |
| | Inverted | −1.00 | −1.13 | −1.25 | −1.20 | −1.13 | −1.1 ± 0.1 |
| D | Upright | 1.05 | 1.20 | 1.30 | 0.85 | 0.89 | 1.1 ± 0.2 |
| | Inverted | −1.48 | −1.14 | −0.99 | −1.12 | −0.99 | −1.1 ± 0.2 |
| E | Upright | 1.13 | 2.59 | 2.96 | 2.06 | 1.88 | 2.1 ± 0.7 |
| | Inverted | −1.84 | −1.57 | −1.70 | −1.30 | −1.05 | −1.6 ± 0.2 |
| | | | | | | Average upright configuration | 1.8 ± 0.4 |
| | | | | | | Average inverted configuration | −1.6 ± 0.3 |
| | | | | | | Cross-film average $d_{33}$ value | 1.7 ± 0.04 |

In order to measure the open circuit voltage of the *DL*-alanine films, wires were attached to the copper substrate with conductive silver paint and connected to a multimeter. Periodic manual compression was applied [12] and the resulting voltages were recorded using a LabVIEW collection routine (Fig. 3). The peak voltage values vary from 190 to 800 mV, with an average output of 480 mV measured over a 40 s period. The maximum value of 800 mV is twice as high as the average voltages generated in phage viruses [31] and $\gamma$-glycine crystals [12] and, for reference, four times as high as the layered 2D material molybdenum disulfide ($MoS_2$) [62]. The variation in peak height and staggered movement from positive to negative is caused by nonuniform release of the film after manual compression and is indicative of material behavior under field environmental stimuli, as opposed to ideal automated compression.

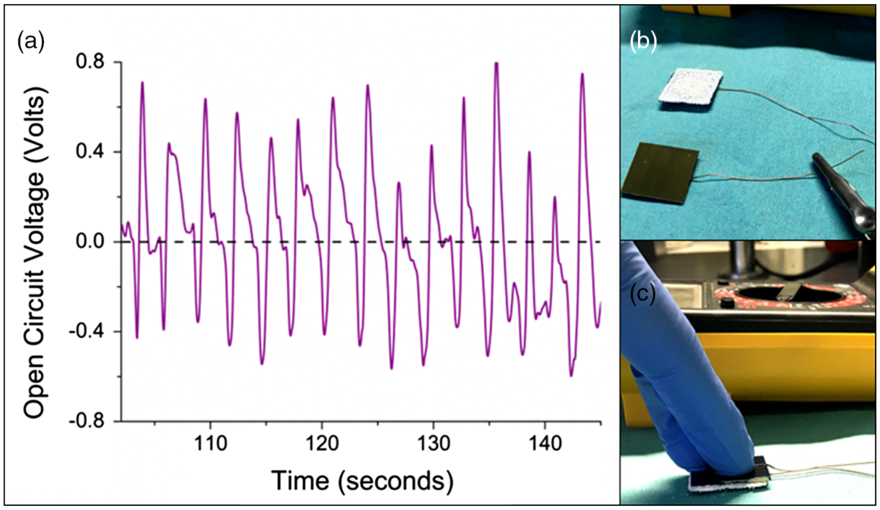

FIG. 3. (a) Open circuit voltage harvested from *DL*-alanine films under periodic manual compression. (b) Racemic amino acid films grown on copper electrodes for energy harvesting tests. (c) Manual compression of *DL*-alanine films between electrodes to generate piezoelectric voltage.

By contrast, *L*-alanine crystals, studied by ourselves [26] and others [40], did not demonstrate the high longitudinal voltages reported in this Letter, even in polycrystalline film form [63]. The validation of longitudinal piezoelectric voltage generation in a *racemic* amino acid crystal allows for high performance stack actuation applications [64] in general consumer electronics and structural health monitoring [65] that have not been possible using previously studied *L*-amino acids.

Given that the measured $d_{33}$ coefficient of the polycrystalline aggregate was, at best, half the predicted $d_{33}$ value for single crystals, we used piezoresponse force microscopy (PFM) to estimate the constant of single crystals of *DL* alanine (Supplemental Material Note 3 and Fig. S4).

Thin isolated single crystals lying parallel to the surface (Fig. S5) were obtained by spin coating (see Supplemental Material [66]), which gave an average $d_{33}$ response of 9.1 pm/V, confirming the accuracy of DFT predictions (for details, see Supplemental Material Note 3 [75]) for single crystals. The PFM measurements also support the hypothesis that the polycrystalline film response is a combined $d_{31}$, $d_{32}$, and $d_{33}$ response, over multiple crystal orientations.

In conclusion, crystal films of *DL* alanine were grown on a variety of substrates, using different deposition methods. Their crystal orientations were characterized and piezoelectrical properties measured using DFT-guided experiments. *DL*-alanine films display an average $d_{33}$ constant of 4.0 pC/N, with maximum responses of up to 4.8 pC/N, at the level of aluminium nitrate single crystals. The crystal properties that confer the large piezoelectric response have been characterized using transmission XRD and SEM of crystal films and DFT calculations and PFM measurements of single crystals. A maximum open circuit voltage of 0.8 V was measured under manual compression, which is twice the maximum previously obtained using amino acid crystals and half that of a dry cell battery.

This publication has emanated from research conducted with the financial support of Science Foundation Ireland (SFI) and is cofunded under the European Regional Development Fund under Grant No. 13/RC/2073. D. T. acknowledges support from SFI under Grant No. 15/CDA/3491 and provision of computing resources at the SFI/Higher Education Authority Irish Center for High-End Computing (ICHEC).

[*]Corresponding author.
sarah.guerin@ul.ie

[1] R. Bechmann, Phys. Rev. **110**, 1060 (1958).
[2] H. Lobl, M. Klee, O. Wunnicke, R. Kiewitt, R. Dekker, and E. Pelt, in *Ultrasonics Symposium (1999); Proceedings of 1999 IEEE* (IEEE, Piscataway, NJ, 1999), p. 1031.
[3] R. Smith and F. Welsh, J. Appl. Phys. **42**, 2219 (1971).
[4] R. Chowdhury, S. Adhikari, and F. Scarpa, Physica (Amsterdam) **42E**, 2036 (2010).
[5] H. Su, A. Strachan, and W. A. Goddard III, Phys. Rev. B **70**, 064101 (2004).
[6] D. Berlincourt and H. Jaffe, Phys. Rev. **111**, 143 (1958).
[7] A. A. Gandhi, M. Wojtas, S. Lang, A. L. Kholkin, and S. A. Tofail, J. Am. Ceram. Soc. **97**, 2867 (2014).
[8] B. Jaffe, *Piezoelectric Ceramics* (Elsevier, New York, 2012), Vol. 3.
[9] P. Ueberschlag, Sensor Review **21**, 118 (2001).
[10] S. Cha *et al.*, Nano Lett. **11**, 5142 (2011).
[11] T. Fett, D. Munz, and G. Thun, Ferroelectrics **274**, 67 (2002).
[12] S. Guerin *et al.*, Nat. Mater. **17**, 180 (2017).
[13] A. Stapleton, M. R. Noor, E. U. Haq, C. Silien, T. Soulimane, and S. A. M. Tofail, J. Appl. Phys. **123**, 124701 (2018).
[14] R. Hinchet and S.-W. Kim, ACS Nano **9**, 7742 (2015).

[15] C. Dagdeviren *et al.*, Proc. Natl. Acad. Sci. U.S.A. **111**, 1927 (2014).

[16] Ensieh Seyedhosseini, Maxim Ivanov, Vladimir Bystrov, Igor Bdikin, Pavel Zelenovskiy, Vladimir Ya. Shur, Andrei Kudryavtsev, Elena D. Mishina, Alexander S. Sigov, and Andrei L. Kholkin, Cryst. Growth Des. **14**, 2831 (2014).

[17] V. Bystrov, E. Seyedhosseini, S. Kopyl, I. Bdikin, and A. Kholkin, J. Appl. Phys. **116**, 066803 (2014).

[18] E. Seyedhosseini, I. Bdikin, M. Ivanov, D. Vasileva, A. Kudryavtsev, B. Rodriguez, and A. Kholkin, J. Appl. Phys. **118**, 072008 (2015).

[19] A. Kholkin, N. Amdursky, I. Bdikin, E. Gazit, and G. Rosenman, ACS Nano **4**, 610 (2010).

[20] C. M. Kelly, T. Northey, K. Ryan, B. R. Brooks, A. L. Kholkin, B. J. Rodriguez, and N.-V. Buchete, Biophys. Chem. **196**, 16 (2015).

[21] Y. Liu, Y. Zhang, M.-J. Chow, Q. N. Chen, and J. Li, Phys. Rev. Lett. **108**, 078103 (2012).

[22] P. Jiang, F. Yan, E. N. Esfahani, S. Xie, D. Zou, X. Liu, H. Zheng, and J. Li, ACS Biomater. Sci. Eng. **3**, 1827 (2017).

[23] Y. Liu, Y. Wang, M.-J. Chow, N. Q. Chen, F. Ma, Y. Zhang, and J. Li, Phys. Rev. Lett. **110**, 168101 (2013).

[24] V. Lemanov, S. Popov, and G. Pankova, Phys. Solid State **53**, 1191 (2011).

[25] S. Guerin, S. A. M. Tofail, and D. Thompson, IEEE Trans. Dielectr. Electr. Insul. **25**, 803 (2018).

[26] S. Guerin, T. A. Syed, and D. Thompson, Nanoscale **10**, 9653 (2018).

[27] P. R. Tulip and S. J. Clark, Phys. Rev. B **74**, 064301 (2006).

[28] P. Tulip and S. Clark, J. Chem. Phys. **121**, 5201 (2004).

[29] Y. Zhang, Y. Bao, D. Zhang, and C. R. Bowen, J. Am. Ceram. Soc. **98**, 2980 (2015).

[30] T. Ikeda, *Fundamentals of Piezoelectricity* (Oxford University Press, New York, 1996).

[31] B. Y. Lee, J. Zhang, C. Zueger, W.-J. Chung, S. Y. Yoo, E. Wang, J. Meyer, R. Ramesh, and S.-W. Lee, Nat. Nanotechnol. **7**, 351 (2012).

[32] L. Fumagalli, D. Esteban-Ferrer, A. Cuervo, J. L. Carrascosa, and G. Gomila, Nat. Mater. **11**, 808 (2012).

[33] T. R. Shrout and S. J. Zhang, J. Electroceram. **19**, 113 (2007).

[34] F. Yu, Q. Lu, S. Zhang, H. Wang, X. Cheng, and X. Zhao, J. Mater. Chem. C **3**, 329 (2015).

[35] L. Persano, C. Dagdeviren, Y. Su, Y. Zhang, S. Girardo, D. Pisignano, Y. Huang, and J. A. Rogers, Nat. Commun. **4**, 1633 (2013).

[36] F. R. Fan, W. Tang, and Z. L. Wang, Adv. Mater. **28**, 4283 (2016).

[37] G. Sa-Gong, A. Safari, S. Jang, and R. Newnham, Ferroelectr. Lett. Sect. **5**, 131 (1986).

[38] V. Lemanov, S. Popov, and G. Pankova, Phys. Solid State **44**, 1929 (2002).

[39] V. Lemanov, Ferroelectrics **238**, 211 (2000).

[40] Z. Tylczyński, A. Sterczyńska, and M. Wiesner, J. Phys. Condens. Matter **23**, 355901 (2011).

[41] See Supplemental Material Table 1 at http://link.aps.org/supplemental/10.1103/PhysRevLett.122.047701 for predicted elastic stiffness constants, $c_{ij}$, and dielectric constants, $\varepsilon_i$, for *DL*-alanine single crystals, calculated using DFT.

[42] T. G. Cooper, W. Jones, W. S. Motherwell, and G. M. Day, CrystEngComm **9**, 595 (2007).

[43] R. Destro, R. Soave, and M. Barzaghi, J. Phys. Chem. B **112**, 5163 (2008).

[44] A. Heredia *et al.*, Adv. Funct. Mater. **22**, 2996 (2012).

[45] D. Isakov, E. d. M. Gomes, I. Bdikin, B. Almeida, M. Belsley, M. Costa, V. Rodrigues, and A. Heredia, Cryst. Growth Des. **11**, 4288 (2011).

[46] R. Ashok Kumar, R. Ezhil Vizhi, N. Vijayan, and D. Rajan Babu, Physica (Amsterdam) **406B**, 2594 (2011).

[47] R. Cook, S. Freiman, B. Lawn, and R. Pohanka, Ferroelectrics **50**, 267 (1983).

[48] A. A. Chernov, J. Struct. Biol. **142**, 3 (2003).

[49] See Supplemental Material Note 1 at http://link.aps.org/supplemental/10.1103/PhysRevLett.122.047701 for optimisation of *DL*-alanine crystal growth, which includes Refs. [50–57].

[50] I. Hod, Y. Mastai, and D. D. Medina, CrystEngComm **13**, 502 (2011).

[51] M. Yamaguchi, F. Miyamaru, K. Yamamoto, M. Tani, and M. Hangyo, Appl. Phys. Lett. **86**, 053903 (2005).

[52] H. A. Levy and R. B. Corey, J. Am. Chem. Soc. **63**, 2095 (1941).

[53] Y. Ma, H. Cölfen, and M. Antonietti, J. Phys. Chem. B **110**, 10822 (2006).

[54] C. Razzetti, M. Ardoino, L. Zanotti, M. Zha, and C. Paorici, Cryst. Res. Technol. **37**, 456 (2002).

[55] N. Vijayan, S. Rajasekaran, G. Bhagavannarayana, R. Ramesh Babu, R. Gopalakrishnan, M. Palanichamy, and P. Ramasamy, Cryst. Growth Des. **6**, 2441 (2006).

[56] H. J. Simpson and R. Marsh, Acta Crystallogr. **20**, 550 (1966).

[57] A. Stapleton, M. Noor, J. Sweeney, V. Casey, A. Kholkin, C. Silien, A. Gandhi, T. Soulimane, and S. Tofail, Appl. Phys. Lett. **111**, 142902 (2017).

[58] See Supplemental Material Note 2 at http://link.aps.org/supplemental/10.1103/PhysRevLett.122.047701 for XRD and SEM characterisation of polycrystalline aggregates, which includes Refs. [59,60].

[59] S. Wohlrab, N. Pinna, M. Antonietti, and H. Cölfen, Chem. Eur. J. **11**, 2903 (2005).

[60] M. Lahav and L. Leiserowitz, Cryst. Growth Des. **6**, 619 (2006).

[61] I. Guy, S. Muensit, and E. Goldys, Appl. Phys. Lett. **75**, 4133 (1999).

[62] W. Wu *et al.*, Nature (London) **514**, 470 (2014).

[63] S. Guerin, S. A. Tofail, and D. Thompson, Cryst. Growth Des. **18**, 4844 (2018).

[64] A. I. Kingon and S. Srinivasan, Nat. Mater. **4**, 233 (2005).

[65] P. Cahill, N. A. N. Nuallain, N. Jackson, A. Mathewson, R. Karoumi, and V. Pakrashi, J. Bridge Eng. **19**, 04014034 (2014).

[66] See Supplemental Material at http://link.aps.org/supplemental/10.1103/PhysRevLett.122.047701 for full experimental and computational details, which includes Refs. [67–74].

[67] J. Hafner, Comput. Phys. Commun. **177**, 6 (2007).

[68] G. Kresse and J. Furthmüller, Phys. Rev. B **54**, 11169 (1996).

[69] G. Kresse and D. Joubert, Phys. Rev. B **59**, 1758 (1999).

[70] N. Argaman and G. Makov, Am. J. Phys. **68**, 69 (2000).

[71] M. Ernzerhof and G. E. Scuseria, J. Chem. Phys. **110**, 5029 (1999).

[72] J. P. Perdew, K. Burke, and M. Ernzerhof, Phys. Rev. Lett. **77**, 3865 (1996).

[73] I. Štich, R. Car, M. Parrinello, and S. Baroni, Phys. Rev. B **39**, 4997 (1989).

[74] X. Gonze and C. Lee, Phys. Rev. B **55**, 10355 (1997).

[75] See Supplemental Material Note 3 at http://link.aps.org/supplemental/10.1103/PhysRevLett.122.047701 for single crystal Piezoresponse force microscopy.